Environmental Research 195 (2021) 110884

Contents lists available at ScienceDirect

Environmental Research

journal homepage: www.elsevier.com/locate/envres

Thermal plasma activation and UV/H_2O_2 oxidative degradation of pharmaceutical residues

Martien H.F. Graumans [a,*], Wilfred F.L.M. Hoeben [b], Maurice F.P. van Dael [a], Rob B.M. Anzion [a], Frans G.M. Russel [c], Paul T.J. Scheepers [a]

[a] Department for Health Evidence, Radboud Institute for Health Sciences, Radboudumc, Nijmegen, the Netherlands
[b] Department of Electrical Energy Systems, Eindhoven University of Technology, Eindhoven, the Netherlands
[c] Department of Pharmacology and Toxicology, Radboud Institute for Molecular Life Sciences, Radboudumc, Nijmegen, the Netherlands

ARTICLE INFO

Keywords:
Advanced oxidation processes
Medicine residues
Complex water matrices
Hospital sewage water

ABSTRACT

The aquatic environment becomes increasingly contaminated by anthropogenic pollutants such as pharmaceutical residues. Due to poor biodegradation and continuous discharge of persistent compounds in sewage water samples, pharmaceutical residues might end up in surface waters when not removed. To minimize this pollution, onsite wastewater treatment techniques might complement conventional waste water treatment plants (WWTPs). Advanced oxidation processes are useful techniques, since reactive oxygen species (ROS) are used for the degradation of unwanted medicine residues. In this paper we have studied the advanced oxidation in a controlled laboratory setting using thermal plasma and UV/H_2O_2 treatment. Five different matrices, Milli-Q water, tap water, synthetic urine, diluted urine and synthetic sewage water were spiked with 14 pharmaceuticals with a concentration of 5 μg/L. All compounds were reduced or completely decomposed by both 150 W thermal plasma and UV/H_2O_2 treatment. Additionally, also hospital sewage water was tested. First the concentrations of 10 pharmaceutical residues were determined by liquid chromatography mass spectrometry (LC-MS/MS). The pharmaceutical concentration ranged from 0.08 up to 2400 μg/L. With the application of 150 W thermal plasma or UV/H_2O_2, it was found that overall pharmaceutical degradation in hospital sewage water were nearly equivalent to the results obtained in the synthetic sewage water. However, based on the chemical abatement kinetics it was demonstrated that the degree of degradation decreases with increasing matrix complexity. Since reactive oxygen and nitrogen species (RONS) are continuously produced, thermal plasma treatment has the advantage over UV/H_2O_2 treatment.

1. Introduction

Aquatic ecosystems are increasingly polluted with anthropogenic compounds such as industrial waste, personal care products, microplastics, pesticides and pharmaceutical residues. Pharmaceutical pollution has received more attention in recent years, due to their effect on the aquatic ecosystem and potential risk for the drinking water quality (Peake et al., 2016; Petrie et al., 2016; Banaschik et al., 2018). Improper disposal, runoff from manure and the continuous excretion from users cause the introduction of pharmaceuticals into the hydrosphere (Magureanu et al., 2015; Souza and Feris 2016; Li et al., 2019). Complete or partially metabolized pharmaceuticals are discharged via domestic and hospital effluents. These effluents are often complex chemical mixtures where pharmaceuticals and metabolites mix with other wastewater ingredients such as soap or other detergents (Beier et al., 2010; Ferrando-Climent et al., 2014; Peake et al., 2016; Ajo et al., 2018). Excreted pharmaceuticals may be metabolized to more bioactive compounds than the administered parent drug. Conventional wastewater treatment plants (WWTPs) cannot completely remove all pharmaceutical residues. Due to continuous discharge and various wastewater treatment technologies, the degradation efficiency for each individual compound will differ from region to region (Peake et al., 2016). Certain WWTPs do convert glucuronide metabolites back into their pristine structure by enzymatic processes (Ajo et al., 2018; Li et al., 2019). Antiepileptics, contrast agents, analgesics, antibiotics and cytostatic drugs are pharmaceutical classes often identified in raw hospital effluents (Beier et al., 2010; Ferrando-Climent et al., 2014; Ajo et al., 2018). To complement and ease conventional WWTPs, onsite

* Corresponding author. P.O. Box 9101, 6500 HB, Nijmegen, (133) Geert Grooteplein-Noord 21, the Netherlands.
E-mail address: martien.graumans@radboudumc.nl (M.H.F. Graumans).

https://doi.org/10.1016/j.envres.2021.110884
Received 23 December 2020; Received in revised form 8 February 2021; Accepted 10 February 2021
Available online 22 February 2021

wastewater treatment techniques are proposed (Gerrity et al., 2010; Banaschik et al., 2015; Ajo et al., 2018). Different techniques such as coagulation-flocculation (Suarez et al., 2009), reverse osmosis (Beier et al., 2010) or advanced oxidation processes (AOPs) (Kohler et al., 2012; Ajo et al., 2018) are studied on pilot-scale to treat hospital wastewater. However, further development of a fully operational on-site treatment technique is often economically too expensive for hospitals to realize (Banaschik et al., 2015; Ajo et al., 2018). AOPs covers the principles of using ROS for the degradation of contaminants by ozone, hydrogen peroxide, peroxone (O_3/H_2O_2) Fenton reaction (Fe^{2+}/H_2O_2), UV, photocatalytic, supercritical and non-thermal gas discharges based oxidative degradation technology (Banaschik et al., 2015; Magureanu et al., 2015; Marković et al., 2015). According to Ajo et al., (2018), plasma treatment is the most efficient technique to produce ROS. In previous studies high degradation efficiencies were observed for pharmaceuticals treated with non-thermal plasma (Banaschik et al., 2018) or the combination of non-thermal plasma with iron as a catalyst (Marković et al., 2015). Plasma-driven activation of water is a new AOP that uses a hot arc (thermal plasma) in air over water to increase both reactive oxygen and nitrogen species (RONS) in water (Hoeben et al., 2019; Graumans et al., 2020). In a previous optimization laboratory-scale experiment we demonstrated that a thermal arc discharged in air over water is capable of the degradation of cyclophosphamide in tap water (Graumans et al., 2020). The aim of the present study was to determine the applicability of thermal plasma to complex matrices. Pharmaceuticals were added to different aquatic matrices, see Fig. 1. Subsequently a generic extraction technique was developed to determine 14 selected compounds. This method was used to analyze

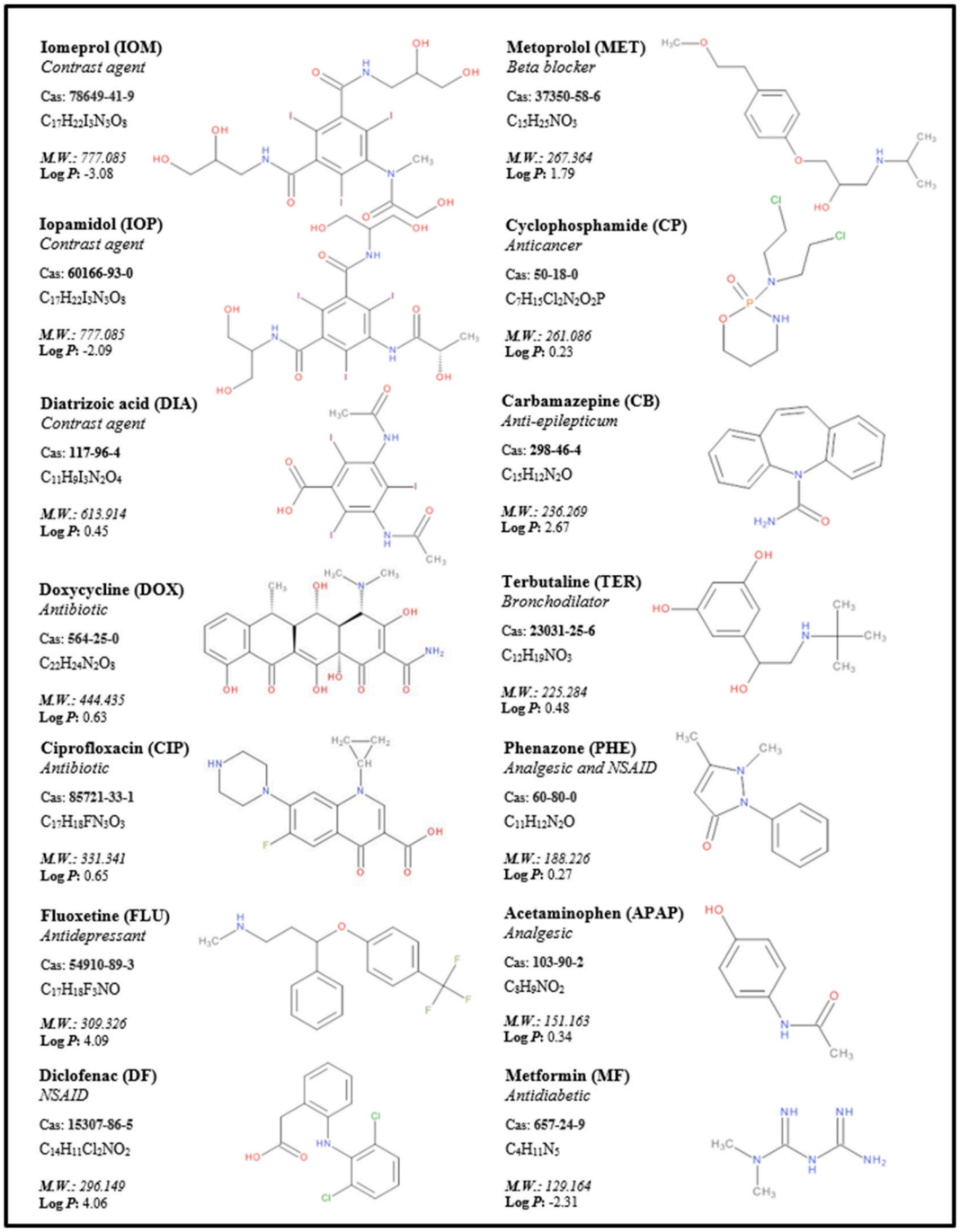

Fig. 1. The 14 selected pharmaceutical compounds, including their classifications and physicochemical properties.

pharmaceutical residues in synthetic and real wastewater matrices such as hospital and domestic sewage water. After analytical determination and characterization of the pharmaceutical residues the hospital effluent was also plasma-treated, to determine the efficacy on real wastewater samples. Due to the wide variety in physicochemical properties of the selected pharmaceuticals, in addition to solid phase extraction, a novel liquid-liquid extraction method for the polar component metformin was developed.

2. Materials and methods

2.1. Chemicals and reagents

Pharmaceutical standards, iopamidol (IOP), diatrizoic acid (DIA), fluoxetine (FLU), diclofenac (DF), metoprolol (MET), carbamazepine (CB), terbutaline (TER), phenazone (PHE), acetaminophen (APAP), ciprofloxacin (CIP), doxycycline (DOX) and metformin (MF), all with >98% purity were retrieved from either Sigma Aldrich/Fluka Analytical (Zwijndrecht, the Netherlands) or Merck Group (Darmstadt, Germany). Endoxan and Iomeron were obtained from Baxter (Utrecht, the Netherlands) and Bracco (Konstanz, Germany) respectively used to prepare a stock solution for cyclophosphamide (CP) and iomeprol (IOM). Mobile phase and buffer solutions were freshly prepared in ultrapure water using a Milli-Q Academic A10 system with a resistivity of 18 MΩ cm (Millipore, Amsterdam the Netherlands). Pharmaceutical stock solutions, with a concentration of 1.0 mg/mL were prepared in 50:50 (v/v) methanol water. Single aliquots of 10.0 μg/mL were subsequently prepared in Milli-Q water and further diluted together to have a pharmaceutical mixture ($n = 14$) with a concentration of 100.0 μg/L. Prior to analysis and solid phase extraction calibration standards were freshly prepared, ranging from 0.5 up to 100.0 μg/L ($n = 6$). Deuterated internal standards (dIS) were all obtained from Toronto Research Chemicals (North York, Canada) and prepared as single stock solutions (1.0 mg/mL) in methanol (SI **paragraph S4**). Compounds needed for the preparation of buffers and simulation matrices included NH_4HCO_2, NaCl, Na_2SO_4, KCl, KH_2PO_4, $CaCl_2 \cdot 2H_2O$, NH_4Cl, K_2HPO_4, $MgSO_4$, sodium dodecyl sulfate, creatine, urea, peptone and meat extract. These chemicals were either acquired from Sigma Aldrich/Fluka Analytical (Zwijndrecht, the Netherlands) or Merck Group (Darmstadt, Germany). UPLC-MS analytical grade chemicals formic acid (FA), methanol (MeOH) and acetonitrile (ACN) were purchased at Merck Group (Darmstadt, Germany) and Boom B.V. (Meppel, the Netherlands) respectively.

2.2. Advanced oxidation processes

2.2.1. Plasma-driven water activation

Thermal plasma discharge was performed using a laboratory-scale plasma activation unit from VitalFluid (Veldhoven, the Netherlands), comprising a 150 W, 1 MHz dual resonant power modulator with 8 kV arc operation voltage, creating a hot arc in air over water (Pemen et al., 2017; Hoeben et al., 2019). A thermal electric discharge with voltages up to 40 kV was generated in air over water. Thermal arc operation was performed in ambient air with a power output of 150 Watt (W). To maintain the temperature of the water during activation between 20 and 35 °C, the plasma unit was equipped with an active Peltier cooler.

2.2.2. UV-C/H_2O_2

Stationary UV-C irradiation was performed by using a modified Aetaire UV air disinfection unit. To irradiate UV-C (Philips PL-L 60 W/4 P HO UV-C lamp, Ekkersrijt, the Netherlands) at 253.7 nm, an opening of 28 cm × 7 cm was used. The distance between the lamp and aqueous matrix surface was approximately 20 cm. At the start of the advanced oxidation process, 0.22 mM (~10 mg/L) hydrogen peroxide (H_2O_2) from J.T. Baker, Avantor Performance Materials (Deventer, the Netherlands) was added. To minimize UV scattering and reflection, a container with an appropriate aperture (12 cm, wide) was placed over the glass beaker. The UV-C irradiance at the aqueous matrix surface was extended and derived from our previous oxidation study (Graumans et al., 2020), (SI **paragraph S1**).

2.3. Simulated aqueous matrices

Thermal plasma and UV-C/H_2O_2 oxidation was applied in Milli-Q, tap water, synthetic urine, diluted urine and synthetic sewage water matrix. All tested aqueous solutions were freshly prepared at the start of the experiment. Milli-Q water was individually tested but also used for the preparation of synthetic urine and synthetic sewage water. A healthy male volunteer consented to provide urine. This urine was diluted to a 20% v/v ratio, in Milli-Q water, to simulate sewer dilution of flushed urine. Physicochemical characteristics of the tap water matrix were adopted from the freely available January–December 2019 quality standard report (Vitens, Arnhem). An average pH of 7.73 was reported, with a total organic carbon (TOC) concentration of <0.5 mg/L and turbidity of 0.24 NTU, detailed information is given in the supplemental data (Table S3). To standardize the advanced oxidation processes, both techniques were used in 500 mL aqueous matrix and during treatment magnetically stirred. The initial pharmaceutical concentration ($n = 14$) was 5 μg/L. The oxidative pharmaceutical degradation was determined by collecting samples at time intervals of 5, 10, 15, 30, 45, 60, 90 and 120 min. Prior to and after oxidative treatment the temperature and pH were measured. Direct LC-MS/MS injection was applied on the matrices, Milli-Q water, tap water and synthetic urine. Sample pre-treatment was applied on diluted urine, synthetic sewage water and actual wastewater samples prior to LC-MS/MS analysis. Centrifugal filtration was used for the urine samples, where solid phase extraction and liquid-liquid extraction were used to pretreat wastewater matrixes.

2.3.1. Synthetic urine

For the preparation of synthetic urine, all needed analytes were dissolved separately in 100 mL Milli-Q, to minimize the formation of precipitation or undissolved constituents. The final product comprises; 25.0 g urea, 2.9 g NaCl, 2.3 g Na_2SO_4, 1.6 g KCl, 1.4 g KH_2PO_4, 1.1 g $CaCl_2 \cdot 2H_2O$, 1.1 g creatinine and 1.0 g NH_4Cl in 1000 mL Milli-Q, simulating human urine composition (Giannakis et al., 2018).

2.3.2. Synthetic sewage

To simulate the composition of sewage water, a standardized protocol from the Organization for Economic Co-operation and Development (OECD) was used. Similar to the preparation of artificial urine, all analytes were prepared separately in 100 mL of Milli-Q. The final synthetic sewage water solution contained; 160.0 mg Peptone, 110.0 mg Meat Extract, 30.0 mg Urea, 28.0 mg K_2HPO_4, 7.0 mg NaCl, 3.0 mg $CaCl_2 \cdot 2H_2O$ and 0.5 mg $MgSO_4$ in 1000 mL Milli-Q water (OECD, 2001).

2.4. Sewage water sample collection

End-of-pipe hospital sewage water (HSW) samples were periodically collected for one week in September 2019 (composite sample). The HSW samples were collected in two separate jerry cans to obtain a sample including the weekend (Thursday – Monday 12–Sep 16, 2019) compared to working days sample (Monday – Thursday 16–Sep 19, 2019). In addition to compare the pharmaceutical concentration present in HSW, also domestic sewage water (DSW) was sampled on Oct 31, 2019 (as a grab sample). These samples were taken from a residential area with no supply of HSW. Upon arrival in the laboratory the wastewater samples were directly centrifuged and vacuum-filtered using a Whatman Filter grade 1 (Maidstone, United Kingdom). The filtered wastewater samples were distributed in separate clean plastic aliquots, labelled and stored in the fridge (4 °C) or freezer (−20 °C). Samples stored in the fridge were analyzed within 72 h to maintain the approximate pharmaceutical shelf

life.

2.5. Centrifugal filtration

To analyze the pharmaceutical oxidative degradation in diluted urine matrix, 0.5 mL urine sample was placed into a Spin-X centrifugal tube from Costar (Salt Lake City, USA). This Spin-X tube is equipped with a 0.22 μm cellulose acetate filter and placed on top of a 2.0 mL tube. To filter the urine sample, an Eppendorf MiniSpin (Nijmegen, the Netherlands) centrifuge is used for 5 min at maximum speed (134000 rpm). After spinning, a clear urine sample was transferred to a LC-MS/MS vial for analysis.

2.6. Solid phase extraction

Acidic buffer solution (ABS) was prepared by dissolving 10 mM of ammonium formate (NH_4HCO_2, ≥99% HPLC grade salt) and 3.25 mL of formic acid (FA, 98–100%) in Milli-Q to obtain a pH of ~2.2. Oasis HLB 3 cc (cm^3) solid phase extraction (SPE) cartridges with 60 mg of solid sorbent from Waters Corporation (Milford, USA), were selected for the extraction. SPE cartridges were conditioned with 2.0 mL of methanol and 2.0 mL of ABS. Prior to analysis, either 1.0 mL of analyte mixture, including 100 μL dIS, HSW or DSW was diluted in 4 mL of ABS. Vacuum extraction was performed using an SPE manifold from Analytichem international (Bay Meadows Ln, USA). An aliquot of 5.0 mL aqueous pharmaceutical matrix was loaded on the SPE cartridge and subsequently washed with 1.0 mL ABS to remove impurities. After sample loading, the retained pharmaceuticals were extracted using 5.0 mL of methanol. Next, the extracts were vaporized under a gentle stream of nitrogen using a sample concentrator (Stuart, Stone, United Kingdom). at 40 °C. The vaporized samples were reconstituted in mobile phase A (0.1% formic acid) prior to LC-MS/MS analysis. To develop an extraction method for pharmaceuticals in a complex matrix in a broad concentration range, the recovery of the selected pharmaceuticals was determined in Milli-Q and synthetic sewage water by using three controlled concentrations, 1.0, 10.0 and 50.0 μg/L.

2.7. Liquid-liquid extraction of metformin

Due to the high hydrophilicity of metformin, no satisfactory recovery was obtained with SPE. To improve the recovery for metformin, a liquid-liquid extraction with acetonitrile at subzero temperatures was performed according to a previously described method (Yoshida and Akane 1999). An aliquot of 0.5 mL of a solution with a known metformin concentration was extracted by adding 0.1 mL of 2.0 mM sodium dodecyl sulfate (SDS) including 0.5 mL of acetonitrile. Sample aliquots were vortexed and centrifuged at maximum speed for 5 min. By placing the tubes for 30 min. at −20 °C, the aqueous phase was separated from the acetonitrile phase. Compounds with affinity for the organic layer were retrieved from the acetonitrile phase. The acetonitrile layer was directly transferred to an LC-MS/MS vial for analysis. For the extraction from actual sewage water, the dimensions were increased by a tenfold, using the ratio 5:1:5 mL (Sewage Water: SDS: Acetonitrile).

2.8. Liquid chromatography tandem mass spectrometry analysis

An Acquity UPLC system from Waters Corporation (Milford, USA) was used for the analytical separation of pharmaceuticals and deuterated internal standards. The LC system was online coupled to a Xevo TQ-S micro quadrupole mass spectrometer, with electro spray ionization (ESI), operated in positive ion mode for all selected compounds. Nitrogen gas was applied at 50 L/h in the cone and at 1100 L/h for desolvation. The desolvation temperature was set at 600 °C, and argon was used as collision gas during MS/MS. The voltages selected for the capillary and cone were 2 kV and 20 V, respectively. Multiple reaction monitoring (MRM) transitions for all pharmaceuticals were determined by direct infusion to the MS/MS. These transitions are presented as a precursor ion $[M+H]^+$ combined with the corresponding fragmented daughter ion. The compounds were all individually infused via the fluidics interface by using a flow rate of 10 μL/min. The optimized results are given in Table S4 (SI **paragraph S4**).

The LC unit consists of a solvent degasser, quaternary solvent manager, seal wash pump, column oven and auto-sampler. Gradient LC conditions were applied at a flow of 0.5 mL/min, using 2.5 μL of injection volume and a column oven temperature set at 40 °C. Eluent (A) consisted of 0.1% v/v formic acid (FA, 98–100%) in Milli-Q water in combination with eluent (B) 100% v/v acetonitrile (ACN, UHPLC-MS). An Acquity UPLC BEH C_{18} (2.1 mm × 100 mm, 1.7 μm) reversed phase column was used for the chromatographic separation. The LC gradient program was started with 100% eluent A until 0.20 min, and quickly changed to 100% B within 2.0 min. This 100% B was maintained until 4.3 min and subsequently ramped to 100% A at 4.5 min. The gradient program was stopped at 8 min.

2.9. Data analysis

For all pharmaceutical compounds the method selectivity was obtained by using two MRM transitions per analyte. For each deuterated internal standard only one MRM transition was selected. Linear curve fitting ($y = ax + b$) was applied using TargetLynx LC-MS/MS data acquisition software (Waters Corporation Milford, USA). Data quantification for metformin (MF) was done by using a quadratic curve fitting ($y = ax^2 + bx + c$). To minimize the y-value error of the low analyte concentrations, all calibration points were equally weighted by using a weighting factor 1/X (Almeida et al., 2002; Gu et al., 2014). The pharmaceutical oxidative degradation kinetics were plotted using GraphPad Prism 5.03 statistical software (Graphpad Inc., CA, USA) and the conversion level was determined using eq. (1) (Graumans et al., 2020). SPE recovery data was determined by dividing the extract concentration through the original concentration, see eq. (2). A *two-sided t*-test was applied to test for statistical significance of degradation over time, assuming first-order kinetics Eq. (3) (Miller and Miller 2010).

$$\overline{R} = (1 - C_t / C_0) \cdot 100\ \% \tag{1}$$

R^{-} = Conversion level (%) ($n = 4$)
C_t = Concentration of the test substance at the end of treatment (μg/L)
C_0 = Initial compound concentration (μg/L)

$$Recovery\ (S\%) = \frac{Concentration\ (Extract)}{Concentration\ (original)} \cdot 100\ \% \tag{2}$$

$$t = \frac{r \cdot \sqrt{n-2}}{\sqrt{1-r^2}} \tag{3}$$

t = *t-calculated*
r^2 = *Correlation coefficient of the log-normal transformed line*

3. Results and discussion

3.1. Pharmaceutical degradation using thermal plasma activation

The oxidative conversion levels of 14 analytes, spiked in five different matrices, were evaluated in a controlled setting. Selected pharmaceuticals at given initial concentrations were degraded by

Table 1
Pharmaceutical removal by thermal plasma treatment in different matrices

Comp.	Milli-Q Water			Tap Water			Synthetic Urine			Urine			Synthetic Sewage		
	$\bar{R}$ (%) $C_{t(min)}$	$\bar{k}$[a] (min^{-1})	$t_{1/2}$ (min)	$\bar{R}$ (%) $C_{t(min)}$	$\bar{k}$ (min^{-1})	$t_{1/2}$ (min)	$\bar{R}$ (%) $C_{t(min)}$	$\bar{k}$ (min^{-1})	$t_{1/2}$ (min)	$\bar{R}$ (%) $C_{t(min)}$	$\bar{k}$ (min^{-1})	$t_{1/2}$ (min)	$\bar{R}$ (%) $C_{t(min)}$	$\bar{k}$ (min^{-1})	$t_{1/2}$ (min)
IOM	66.9	0.009	77.0	62.2	0.007	99.0	43.1	0.005	138.6	25.1	0.002	346.6	56.3	0.008	86.6
	120	*0.96 r^2*		*120*	*0.84 r^2*		*120*	*0.93 r^2*		*120*	*0.73 r^2*		*120*	*0.93 r^2*	
IOP	63.0	0.008	86.6	47.1	0.005	138.6	0.0	-	-	35.5	0.003	231.1	33.1	0.007	99.0
	120	*0.99 r^2*		*120*	*0.89 r^2*		-	-		*120*	*0.48 r^{2b}*		*120*	*0.75 r^2*	
DIA	41.3	0.004	173.3	31.8	0.003	231.1	30.7	0.003	231.1	5.9	<0.001	>693.2	15.3	0.002	346.6
	120	*0.97 r^2*		*120*	*0.89 r^2*		*120*	*0.91 r^2*		*120*	*0.02 r^{2b}*		*120*	*0.51 r^2*	
CIP	99.4	0.030	23.1	72.2	0.006	115.5	68.6	0.006	115.2	81.6	0.015	46.2	69.6	0.013	53.3
	120	*0.67 r^2*		*120*	*0.29 r^{2b}*		*120*	*0.64 r^2*		*120*	*0.97 r^2*		*120*	*0.97 r^2*	
DOX	100.0	0.032	21.7	100.0	0.030	23.1	100.0	0.041	16.9	81.9	0.013	53.3	100.0	0.059	11.8
	90	*0.85 r^2*		*120*	*0.83 r^2*		*90*	*0.83 r^2*		*120*	*0.84 r^2*		*90*	*0.96 r^2*	
FLU	82.8	0.017	40.8	81.2	0.014	49.5	70.2	0.010	69.3	67.6	0.010	69.3	82.5	0.016	43.3
	120	*0.98 r^2*		*120*	*0.97 r^2*		*120*	*0.99 r^2*		*120*	*0.98 r^2*		*120*	*0.96 r^2*	
DF	100.0	0.520	1.3	100.0	0.295	2.4	100.0	0.108	6.4	100.0	0.097	7.1	99.1	0.026	26.7
	15	*1.00 r^2*		*15*	*1.00 r^2*		*15*	*1.00 r^2*		*45*	*0.96 r^2*		*120*	*0.58 r^2*	
MET	72.3	0.011	63.0	61.7	0.008	86.6	49.6	0.005	138.6	9.6	<0.001	>693.2	64.7	0.009	77.0
	120	*0.99 r^2*		*120*	*0.98 r^2*		*120*	*0.98 r^2*		*120*	*0.11 r^2*		*120*	*0.96 r^2*	
CP	100.0	0.160	4.3	100.0	0.185	3.8	100.0	0.078	8.9	100.0	0.049	14.2	100.0	0.121	5.7
	120	*0.98 r^2*		*60*	*0.91 r^2*		*60*	*0.97 r^2*		*90*	*0.82 r^2*		*90*	*0.97 r^2*	
CB	90.5	0.019	36.5	84.4	0.019	36.5	62.3	0.008	86.6	37.9	0.004	173.3	79.4	0.014	49.5
	120	*0.99 r^2*		*120*	*0.99 r^2*		*120*	*0.98 r^2*		*120*	*0.93 r^2*		*120*	*0.97 r^2*	
TER	92.7	0.021	33.0	95.2	0.046	15.1	89.5	0.018	38.5	91.9	0.021	33.0	85.3	0.016	43.3
	120	*0.98 r^2*		*120*	*0.95 r^2*		*120*	*0.95 r^2*		*120*	*0.99 r^2*		*120*	*0.98 r^2*	
PHE	100.0	0.149	4.7	100.0	0.192	3.6	100.0	0.207	3.4	100.0	0.059	11.8	100.0	0.263	2.6
	30	*0.70 r^2*		*30*	*0.75 r^2*		*30*	*0.98 r^2*		*90*	*0.91 r^2*		*45*	*0.97 r^2*	
APAP	100.0	0.774	0.9	100.0	0.115	6.0	100.0	0.271	2.6	100.0	0.065	10.7	100.0	0.739	0.94
	15	*1.00 r^2*		*30*	*1.00 r^2*		*45*	*0.97 r^2*		*60*	*0.98 r^2*		*30*	*1.00 r^2*	
MF	17.6	0.001	693.2	42.8	0.004	179.3	0.0	-	-	29.3	0.003	231.1	72.9	0.011	63.0
	120	*0.94 r^2*		*120*	*0.74 r^2*		-	-		*120*	*0.82 r^2*		*120*	*0.71 r^2*	

[a] First-order reaction rate equation: $-d[A]/dt = k$, the first-order rate constant, is the slope of the line. Where **[A]** is the drug concentration and $t_{(1/2)} = \ln 2/k$
[b] No significant change due to moderate to low correlation coefficient in linear modelling of assumed first-order kinetics ($r^2 < 0.50$).

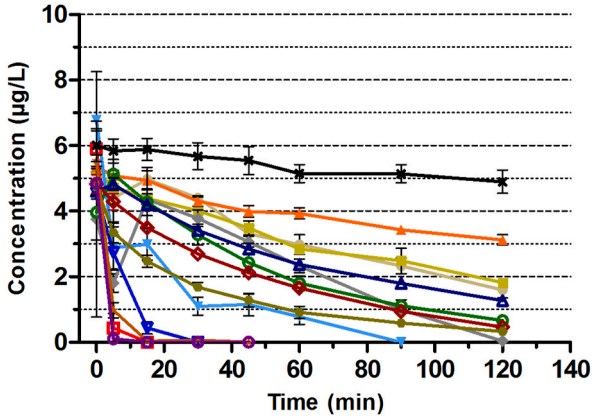

Fig. 2. The time-based decomposition plot for the pharmaceuticals **IOM** (●), **IOP** (■), **DIA** (▲), **CIP**(◆), **DOX** (▼), **FLU**(○), **DF** (□), **MET** (△), **CP**(▽), **CB**(◇), **TER** (●), **PHE**(★), **APAP** (○) and **MF**(✖), treated in Milli-Q water with 150 W thermal plasma.

oxidation to an energy density and compound dependent extent using 150 W thermal plasma treatment, (Table 1). Milli-Q was used as ultra-pure water matrix where all molecules are solely oxidized by plasma-generated RONS. A time-based decomposition plot demonstrates that the chemical degradation kinetics are distinct for all analytes tested, see Fig. 2. DOX, DF, CP, PHE and APAP were all rapidly 100% decomposed, with similar abatement kinetics. The compounds CIP, FLU, CB and TER were converted for at least >90% within 120 min. The slowest degradation was observed for MET (72.3%), IOM (66.9%), IOP (63.0%), DIA (41.3%) and MF (17.6%) after 120 min treatment. Although the chemical degradation kinetics differ between compounds and matrices, during thermal plasma treatment the analytes were observed to be subjected to exponential decay. Log-normal transformation of this concentration data resulted in linear time-based decomposition plots, see Fig. S5 (SI **paragraph S5**). The slope of this linear decay represents the first-order rate constant (k) where $r^2 > 0.50$ demonstrates significant correlation for first-order degradation kinetics (SI **paragraph S5**).

Comparison of the pharmaceutical degradation rate constants in Milli-Q with other matrices (Table 1 and Fig. S3 and 4 (SI **paragraph S5**)), it is demonstrated that the k value decreases with increasing matrix complexity. To demonstrate the influence of co-existing substances present in these treated matrices, the overall rate constant ($\bar{k}$) was used to calculate the inhibition ratio, see eq. (4) (Tokumura et al., 2016). A ratio higher than 1.000 suggests inhibition by constituents and organic matter in the sample matrix indicating that the aqueous composition is of major influence on plasma oxidation efficiency. The matrix complexity and interference of co-existing substances was consecutively demonstrated to be:

$$1.000_{(Milli-Q)} < 1.344_{(Synthetic\ \ Sewage)} < 1.893_{(Tap\ \ water)} < 2.119_{(Synthetic\ \ urine)} < 5.000_{(Urine)}.$$

$$\text{Inhibition ratio} = \frac{k_{(Milli-Q)}}{k_{(Matrix)}} \quad (4)$$

It is demonstrated that the aqueous composition is of great influence on the plasma oxidation efficiency. Despite the overall inhibitory effect of co-existing substances in various tested media, synthetic sewage and tap water, compared to Milli-Q, showed improved degradation rate constants for DOX, CP, TER, PHE and MF. The relatively small improvement in degradation for these compounds is attributed to matrix conductivity. Enhanced conductivity will increase the ability of facilitating electrical current through an aqueous medium, suggesting that the pre-existence of ions in tap water and synthetic sewage accelerate the transfer of specific RONS (Brisset et al., 2011; Thirumdas et al., 2018; Hoeben et al., 2019; Shimizu et al., 2020). Increased solution conductivity also increases the current of the thermal plasma arc, promoting the chemical activity of the plasma discharge in the gas phase. A similar effect would have been expected in synthetic and diluted urine matrices, however, an inhibitory effect was observed. This effect is probably explained by the high concentration of the co-existing minerals and organic constituents present in g/L ranges compared to mg/L range in tap water and synthetic sewage water (OECD, 2001; Giannakis et al., 2018). Shih and Locke (2011) demonstrated in their study an optimal conductivity of 150 μS/cm for the production of reactive species. Further increase of conductivity (up to 500 μS/cm) resulted in a decline of radicals and molecular species formed. Due to the presence of co-existing substances there is less direct contact with water molecules to produce hydroxyl radicals (**R1**). On the other hand minerals and organic constituents may cause quenching or the production of less reactive radicals (Shih and Locke 2011; Giannakis et al., 2018; Shimizu et al., 2020). Slower and no gradual abatement kinetics was therefore also observed in urine diltued with water, showing a poor correlation of $r^2 < 0.50$ for the degradation of IOP (0.48 r^2), DIA (0.02 r^2) and MET (0.11 r^2).

3.2. Plasma oxidation chemistry

Many factors can influence thermal plasma degradation efficiency. In our previous study we observed that electrical power input and initial analyte concentration were important parameters (Graumans et al., 2020). Additionally, it was demonstrated that by continued activation of a relatively large volume of tap water (500 mL) and low pharmaceutical concentration (4 μg/L), a logistic oxidative degradation pattern for CP elapsed. Comparing the previously non-cooled plasma results with the current data, no logistic oxidative degradation pattern is found for CP and other treated analytes, see Fig. S6 (SI **paragraph S6**). This remarkable dissimilarity is attributed to the temperature of the plasma treated solution. Active cooling has a positive effect on the production of thermally labile species such as ozone, hydrogen peroxide and transient reactive nitrogen species, while high temperatures benefit nitric acid formation (Hoeben et al., 2019). Hydroxyl radicals (HO•) and their coupling product hydrogen peroxide (H_2O_2) are formed by plasma-water contact, either in the gas phase or at the plasma-water interface (**R1**) (Joshi and Thagard 2013). Two HO• radicals combine to form measurable hydrogen peroxide concentrations (**R2**) (Magureanu et al., 2018). On the other hand, in presence of organic molecules, such as pharmaceuticals HO• radicals will react by initiating oxidative degradation (Joshi and Thagard 2013; Magureanu et al., 2018).

$$e^- + H_2O \rightarrow OH^\bullet + H + e^- \quad (R1)$$

$$HO^\bullet + HO^\bullet \rightarrow H_2O_2 \quad (R2)$$

Pharmaceutical decomposition initiated by HO• radicals produced with immersed non-thermal pulsed corona plasma, was demonstrated before (Banaschik et al., 2018). Oxidative conversion levels for three identical compounds in Milli-Q were found for DIA (40%), DF (100%) and CB (75%) within 70 min. We observed decomposition levels of 41.3%, 100% and 90.5% within 120 min for DIA, DF and CB, respectively. Although the oxidative degradation of these pharmaceuticals shows similarities, it must be noted that the plasma degradation in our study is not solely based on hydroxyl radical interaction. With plasma discharge in ambient air and striking over water, also reactive nitrogen species are transferred in the liquid matrix (Hoeben et al., 2019; Graumans et al., 2020), such as nitric oxide (NO), nitrogen dioxide (NO_2), nitrous acid (HNO_2), nitric acid (HNO_3) and peroxynitrous acid (ONOOH). In addition to oxidative degradation, these RNS can also induce nitration and nitrosation reactions (Magureanu et al., 2018; Hoeben et al., 2019). Looking at the currently tabulated conversion levels (R^-) and corresponding half-lives ($t_{1/2}$), (Table 1), it is clear that certain molecular structures are more suspectable to plasma produced RONS than others. Aromatic ring systems, unsaturated double bonds (C = C) and functional groups with electron donating properties have increased reactivity towards electrophilic oxidizing agents (HO• or NO_2^+) (Brown, 2007; Joshi and Thagard 2013; Banaschik et al., 2018; Magureanu et al., 2018). The reactivity of aromatic ring systems is however, not self-evident since an electrophile, such as a hydroxyl radical, is needed to interact (Brown, 2007).

A technology such as plasma-induced water activation is used to generate electrophilic compounds, demonstrating that HO• radicals readily initiate an addition reaction by binding to an aromatic ring system, Fig. 3A. (Banaschik et al., 2018). A similar reaction pathway is expected during our thermal plasma treatment process, but are complemented by nitration processes (Magureanu et al., 2018; Hoeben et al., 2019; Graumans et al., 2020). With prolonged thermal plasma activation, the aqueous matrix pH is decreased by RONS (Table 2). Nitration reactions usually occur at acidic pH (<6), where a nitronium ion (NO_2^+) is substituted or added as an electrophile at the aromatic ring system (Squadrito and Pryor 1998; Brown, 2007). Chiron et al., (2010), identified 3-nitro-APAP as the nitration transformation product of APAP in WWTPs (Chiron et al., 2010), see Fig. 3B. Nitration reactions in WWTP are initiated by nitrifying bacteria who produce nitric oxide (NO•). NO• is a precursor for nitrating agents such as peroxynitrite ($ONOO^-$). In acidic samples ONOOH is very unstable and will rapidly decompose into HO•, NO_2 and HNO_3 (Chiron et al., 2010; Jewell et al., 2014; Hoeben et al., 2019). Additionally, $ONOO^-$ can also react with CO_2 yielding $NO_2^\bullet$ and $CO_3^{\bullet-}$ radicals (Chiron et al., 2010). For thermal plasma activation it is expected that similar RONS are produced (**R3-6**). However, it is expected that the combined attack of hydroxyl radical and molecular oxygen is the main degradation pathway in this thermal plasma study and that nitration oxidation will complement the oxidative process under favorable circumstances (Chiron et al., 2010; Jewell et al., 2014; Thirumdas et al., 2018; Magureanu et al., 2018; Hoeben et al., 2019).

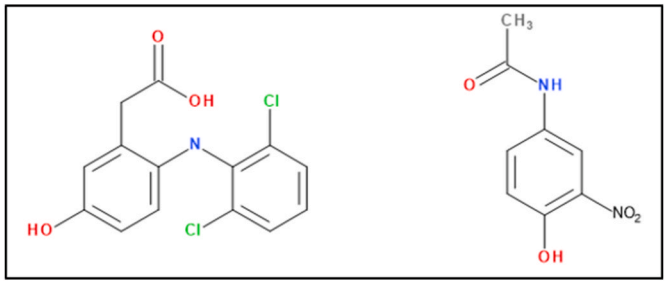

Fig. 3. During thermal plasma treatment distinct chemical processes will occur according to the produced RONS. Several RONS will initiate chemical processes on reactive molecular structures containing aromatic rings, unsaturated bonds or electron donating function groups. HO• radical attack is the favored degradation pathway, reacting for example rapidly with the aromatic ring of DF by forming 4-hydroxy-DF **(A)**. Additionally, nitration processes will also occur where for example $NO_2^\bullet$ radicals can add to aromatic ring of APAP by producing 3-nitro-APAP **(B)**.

Table 2
Average pH values of $n = 2$ thermal plasma treated matrices.

150W Plasma	Milli-Q Water pH x⁻	Tap Water pH x⁻	Synthetic Urine pH x⁻	Urine pH x⁻	Synthetic Sewage pH x⁻
Start $_{0\ min}$	5.0	7.7	6.5	7.4	6.9
End$_{120\ min}$	1.6	1.6	2.2	2.5	1.7

Our previous study on degradation data of CP without active cooling indicated pharmaceutical dissolution after prolonged activation (Graumans et al., 2019). This suggests that minimal HO• radicals were formed, but that molecular dissolution was catalyzed by acidic pH (<6) and increasing water temperature, both acting as stimulants for the nitration reaction rate (Chiron et al., 2010).

$$e^- + N_2 \rightarrow N^\bullet + N^\bullet + e^- \quad \text{(R3)}$$

$$N^\bullet + O_2 \rightarrow NO^\bullet + O^\bullet \quad \text{(R4)}$$

$$NO^\bullet + O_2^{\bullet-} \rightarrow \mathrm{ONOO^-} \quad \text{(R5)}$$

$$ONOO^- + H^+ \rightarrow NO_2^\bullet + HO^\bullet \quad \text{(R6)}$$

3.3. UV-C/H_2O_2 oxidative chemistry

UV-C/H_2O_2 advanced oxidation process is another useful technique for the degradation of micropollutants such as pharmaceuticals (Wols et al., 2013). During the application with UV-C/H_2O_2 treatment, certain molecules are sensitive for both interactions and are rapidly converted by photolysis and hydroxyl radical attack (Wols et al., 2013). Hydrogen peroxide in the gas phase is rapidly dissociated by UV photons, producing highly reactive hydroxyl radicals (•OH) that can interact with nearly all organic compounds (von Sonntag 2008; Zhao et al., 2014).•OH radicals will bind to C = C or C = N double bonds, initiate hydrogen (H) abstraction, or trigger electron transfer reactions (von Sonntag 2008; Banaschik et al., 2018). According to the degradation results (Fig. 4.), it is seen that UV-C/H_2O_2 attacks nearly all pristine molecular structures completely in Milli-Q water, Table 3. Pseudo first-order reaction kinetics ranged between 0.007 up to 0.591 min^{-1}, including corresponding half-lives ($t_{1/2}$) between 0.4 and 99.0 min. In contrast to thermal plasma treatment, the complete conversion of IOM, IOP and DIA with UV-C/H_2O_2 is most remarkable, since the molecular reactivity of these molecules is relatively low (Bourin et al., 1997). DIA is weak acidic compound, where IOM and IOP are both nonionized over a wide pH range, see Table S5 (SI **paragraph S7**).

The fully substituted aromatic ring with iodine atoms is characteristic for contrast agents, since these structures facilitate X-ray absorption during clinical diagnosis (Bourin et al., 1997; Borowska et al., 2015). That these compounds are difficult to decompose during plasma oxidation is explained by the fully substituted aromatic ring, where the iodine functional groups hinder the availability of the unsaturated C-atoms (Rosati 1994; Bourin et al., 1997; Zhao et al., 2014; Banaschik et al., 2018). Assuming that hydroxyl radical attack is the major pathway during thermal plasma degradation study, it confirms that slow molecular invasion can occur (Banaschik et al., 2018). On the other hand it is noteworthy, that the hydroxyl radical can attack on the ipso positions of the aromatic ring, as observed with e.g. DIA, IOP and IOM (Jeong et al., 2010). Despite their slow chemical reactivity towards HO• radicals, iodinated compounds are light sensitive Photolysis of these molecules causes deiodination (Eloy et al., 1991; Wols et al., 2013). Allard et al., (2016) demonstrated rapidly photolytically degraded IOP and DIA up to >90% within 2 min in deionized water by immersed UV irradiation at 254 nm (Allard et al., 2016). Although we use UV/H_2O_2 treatment, similar fast complete conversion levels were found for IOM, IOP and DIA within 15 min, demonstrating that the used UV-C source (254 nm) is the most important technique for contrast agent degradation. In accordance with the study of Wols, we found that the majority of pharmaceuticals do not photolytically degrade at 254 nm UV irradiation. Based on their data it was seen that DF, PHE and FLU can moderately decompose photolytically in Milli-Q, where MET, CP, CB, APAP and MF are scarcely sensitive to UV-C irradiation (Wols et al., 2013). The poorest conversion levels were observed for APAP, CP and MF. Although UV-C/H_2O_2 treatment is an interplay between photochemical degradation accompanied with HO• radicals, we found that UV-C irradiation has a large impact on the molecular degradation.

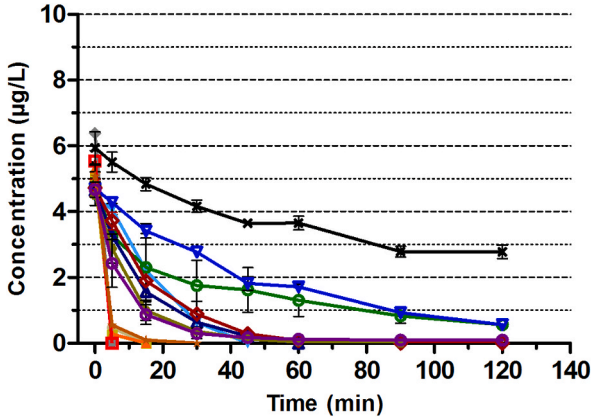

Fig. 4. UV-C/H_2O_2 oxidative degradation pattern in Milli-Q for the compounds **IOM** (●), **IOP** (■), **DIA** (▲), **CIP**(◆), **DOX** (▼), **FLU**(○), **DF** (□), **MET** (△), **CP**(▽), **CB**(◇), **TER** (●2), **PHE**(★), **APAP** (○) and **MF**(✖).

3.4. Effect of complex matrices on UV-C/H_2O_2 treatment

Also during UV-C/H_2O_2 oxidative treatment the matrix complexity has a significant effect on the oxidative degradation of molecules. Using again the inhibition factor (Eq. (4)), it has been observed that the coexisting substances in the aqueous matrix have even a greater influence on UV-C/H_2O_2 oxidation than during plasma treatment. The pharmaceutical degradation kinetics (Table 3) decrease when the matrix complexity increases:

$$1.000_{(Milli-Q)} : \ 0.544_{(Tap\ water)} < 3.115_{(Synthetic\ Sewage)} < 15.283_{(Synthetic\ urine)} < 54.00(Urine).$$

The rapid conversion levels in Milli-Q are presumably caused by the absence of minerals and organic impurities. Retardation of the chemical degradation kinetics in complex matrices like synthetic urine, diluted urine and synthetic sewage are attributed to minerals and the natural organic matter. Organic impurities, such as urea, meat extract and peptone will absorb UV light at the expense of a less effective photolytic process. Indirectly the production of HO• radicals is also diminished and minerals such as phosphate and chlorine will induce the production of less reactive secondary radicals (**R7-8**) (Borowska et al., 2015; Giannakis et al., 2018).

$$HO^\bullet + Cl^- \rightarrow HOCl^{\bullet-} \quad \text{(R7)}$$

$$HO^\bullet + HPO_4 \rightarrow HPO_4^{\bullet-} + HO^- \quad \text{(R8)}$$

On the other hand, it was observed that the MF oxidation is increased in tap water. Chemical degradation kinetics are improved in tap water matrix (0.028 min^{-1}) compared to Milli-Q (0.007 min^{-1}), showing 97.4% versus 52.9% degradation within 120 min, respectively. This effect is attributed to photoreactive NO_3^- (Lin et al., 2020), and in this study also improved degradation of MF was demonstrated in water

Table 3
Pharmaceutical removal by UV-C/H_2O_2 treatment in different matrices.

	Milli-Q Water			Tap Water			Synthetic Urine			Urine			Synthetic Sewage		
	R^- (%) $C_{t(min)}$	k (min^{-1})	$t_{1/2}$ (min)	R^- (%) $C_{t(min)}$	k (min^{-1})	$t_{1/2}$ (min)	R^- (%) $C_{t(min)}$	k (min^{-1})	$t_{1/2}$ (min)	R^- (%) C_t (min)	k (min^{-1})	$t_{1/2}$ (min)	R^- (%) $C_{t(min)}$	k (min^{-1})	$t_{1/2}$ (min)
IOM	100.0	0.477	1.6	100.0	0.464	1.5	80.7	0.014	49.0	43.7	0.005	138.6	100.0	0.124	5.6
	15	*1.00 r^2*		*15*	*1.00 r^2*		*120*	*0.97 r^2*		*120*	*0.58 r^2*		*30*	*0.99 r^2*	
IOP	100.0	0.587	1.2	100.0	0.361	1.9	85.3	0.015	46.2	53.2	0.007	99.0	100.0	0.101	6.9
	15	*1.00 r^2*		*15*	*1.00 r^2*		*120*	*0.98 r^2*		*120*	*0.84 r^2*		*30*	*0.99 r^2*	
DIA	100.0	0.591	1.2	100.0	0.848	0.8	86.3	0.018	38.5	39.8	0.005	138.6	100.0	0.126	5.5
	15	*1.00 r^2*		*15*	*1.00 r^2*		*120*	*0.97 r^2*		*120*	*0.88 r^2*		*30*	*0.98 r^2*	
CIP	100.0	n/a[a]	–	100.0	0.292	2.4	86.2	0.015	46.2	8.6	0.001	693.2	100.0	0.159	4.4
	15	-		*30*	*0.99 r^2*		*120*	*0.95 r^2*		*120*	*0.44 r^2 **		*60*	*0.99 r^2*	
DOX	100.0	0.067	10.4	n.d.	–	–	60.5	0.007	99.0	23.8	0.003	231.1	83.0	0.014	49.5
	45	*0.97 r^2*		-	–		*120*	*0.86 r^2*		*120*	*0.44 r^2 **		*120*	*0.92 r^2*	
FLU	87.9	0.016	43.3	100.0	0.109	6.4	62.5	0.008	86.6	18.5	0.002	346.6	94.8	0.027	25.7
	120	*0.95 r^2*		*60*	*0.86 r^2*		*120*	*0.99 r^2*		*120*	*0.85 r^2*		*120*	*0.84 r^2*	
DF	100.0	n/a[a]	–	100.0	1.853	0.4	100.0	0.046	15.1	69.7	0.010	69.3	99.3	0.036	19.3
	15	-		*15*	*1.00 r^2*		*120*	*0.97 r^2*		*120*	*0.99 r^2*		*120*	*0.56 r^2*	
MET	100.0	0.068	10.2	97.3	0.043	16.1	12.1	0.001	693.2	3.7	0.002	346.6	46.1	0.005	138.6
	60	*0.99 r^2*		*120*	*0.99 r^2*		*120*	*0.85 r^2*		*120*	*0.59 r^2*		*120*	*0.90 r^2*	
CP	87.9	0.018	38.5	53.2	0.017	40.8	4.6	n.d.	–	6.6	<0.001	>693.2	17.8	0.001	693.2
	120	*0.99 r^2*		*120*	*0.99 r^2*		*120*	-		*120*	*0.39 r^2 **		*120*	*0.54 r^2*	
CB	100.0	0.075	9.2	88.5	0.019	99.0	8.1	0.001	693.2	N.C.	–	–	27.9	0.003	231.1
	120	*0.99 r^2*		*120*	*0.99 r^2*		*120*	*0.36 r^2 **		–	–		*120*	*0.81 r^2*	
TER	100.0	0.079	8.8	100.0	n.d.	–	53.1	0.005	138.6	4.1	<0.001	>693.2	70.7	0.009	77.0
	90	*0.99 r^2*		*15*	-		*120*	*0.92 r^2*		*120*	*0.05 r^2 **		*120*	*0.98 r^2*	
PHE	100.0	0.249	2.8	100.0	0.013	1.6	78.5	0.013	53.3	35.0	0.004	173.3	100.0	0.110	63.0
	30	*0.93 r^2*		*45*	*0.99 r^2*		*120*	*0.99 r^2*		*120*	*0.92 r^2*		*120*	*0.99 r^2*	
APAP	97.8	0.031	22.4	100.0	0.127	5.5	24.1	0.002	346.6	N.C.	–	–	70.1	0.009	77.0
	120	*0.75 r^2*		*30*	*0.91 r^2*		*120*	*0.95 r^2*		–	–		*90*	*0.95 r^2*	
MF	52.9	0.007	99.0	97.4	0.028	24.8	40.7	0.003	231.1	11.3	0.001	693.2	9.6	0.002	346.6
	120	*0.92 r^2*		*120*	*0.73 r^2*		*120*	*0.52 r^2*		*120*	*0.68 r^2*		*120*	*0.47 r^2 **	

*: No significant change due to moderate to low correlation coefficient in linear modelling of assumed first-order kinetics ($r^{2\ leg} < 0.50$).
[a] No reaction rate could be determined, by the rapid interaction of the pharmaceutical with either H_2O_2 or UV-C irradiation.

samples with amplified environmental factors, compared to pure water. Their experimental design was based on simulating environmental photolysis by using 6 h of UV-A irradiation at 40 cm distance. During this process, reactive oxygen species (ROS) are formed confirming that HO• radical attack is the favored MF degradation pathway (Lin et al., 2020). Improved degradation results were found in the presence of high concentrations NO_3^- (0.60–0.62 mg/L) and to a lesser extent Cl^- (up to <4 mg/L), which both promote the photo-reactivity by producing HO• radicals (**R9-R11**) (Wang et al., 2017; Lin et al., 2020) As seen in the suggested chemical reactions, it is expected that primarily NO_2 and NO_3

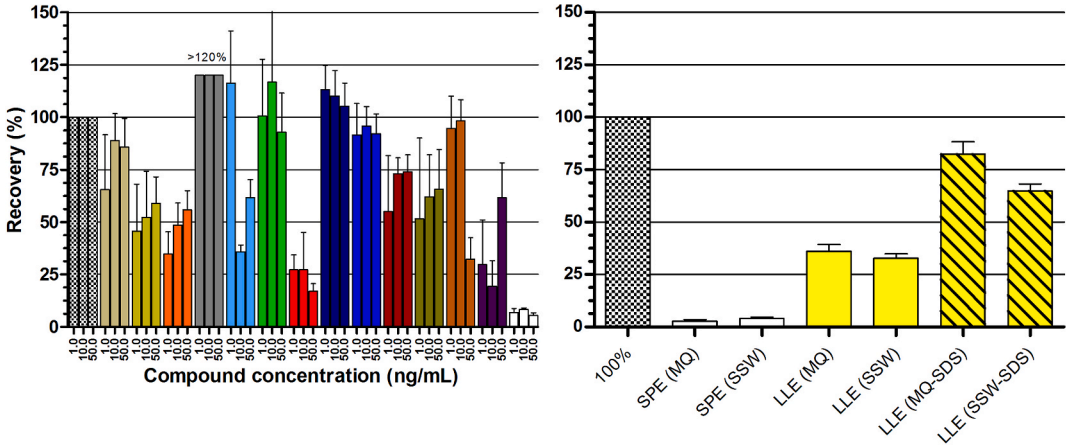

Fig. 5. SPE recovery percentages obtained in spiked synthetic sewage water (**A**). The extraction of known concentrations 1.0, 10.0 and 50.0 μg/L is compared to **100%(■6)** recovery for the compounds; **IOM** (■), **IOP** (■), **DIA** (■), **CIP**(■), **DOX** (■), **FLU**(■), **DF** (■), **MET** (■), **CP**(■), **CB**(■5), **TER** (■), **PHE**(■), **APAP** (■) and **MF** (□). Liquid-liquid extraction compared to SPE extraction (**B**). Recovery was determined for 50 μg/L **MF**(□9), without (■) and with SDS (▨).

will play an improved role in UV-C/H_2O_2 tap water. As demonstrated in Table S3 (SI **paragraph S3**), it is seen that both Cl_2 and NO_3 are present in concentrations exceeded the threshold of <4.0 mg/L (Lin et al., 2020).

$$NO_3^- \xrightarrow{UV} NO_3^{-*} \quad \text{(R9)}$$

$$NO_3^{-*} \rightarrow NO_2^{\bullet} + O^- \quad \text{(R10)}$$

$$O^- + H_2O \rightarrow HO^{\bullet} + HO^- \quad \text{(R11)}$$

3.5. Pharmaceutical extraction using solid phase extraction and liquid-liquid extraction

A versatile SPE methodology was developed in synthetic sewage water for the detection of 14 different pharmaceuticals in raw hospital and residential wastewater samples. The extraction method was developed and optimized for synthetic sewage water to achieve an optimum recovery in a sterile matrix with comparable properties as raw wastewater. Due to the wide range of physicochemical properties of our selected pharmaceuticals ($n = 14$), the current developed SPE and LLE methodology are a compromise to achieve the best overall extraction efficiency, see supporting information **paragraph S8** for the detailed results. The currently developed SPE methodology has recovery percentages (S%) ranging from 27 up to > 100.0% for 13 pharmaceuticals in synthetic sewage water, see Fig. 5.

The extraction of MF, was insufficient, since recovery percentages using Oasis HLB SPE cartridges were very low (S% >10.0). To minimize LC-MS/MS system contamination or have any recovery loss of other pharmaceuticals, an additional liquid-liquid extraction at subzero temperatures from Yoshida et al. (1999) was modified especially for MF (Yoshida and Akane 1999). SDS was added to the sample to initiate a cation-anion interaction between MF and SDS. ACN was added to extract the SDS-MF complex from the aqueous matrix. As presented in Fig. 5B, it is seen that the LLE method can extract MF now with much better recovery, ranging from 64.9 up to ~100%.

3.6. Pharmaceutical detection and mitigation

The optimized SPE and LLE extraction methods were used on real wastewater samples taken from a hospital and residential area (Fig. 6). The concentrations (μg/L) of the 10 identified pharmaceuticals were comparable with other studies of Vieno et al. (2006); Yin et al. (2010), Petrie et al. (2016) and Ajo et al. (2018). Results reported for IOM and APAP are considered semi-quantitative because these values were extrapolated in a range beyond the highest standard concentration (100 μg/L). Even with this limitation of our analytical method, nearly all 14 selected pharmaceuticals were detected in the hospital effluent (Table 4). The presence of IOM, DIA and CP, illustrates the difference between hospital (HSW) and domestic sewage water (DSW), since contrast agents and certain anticancer drugs are hospital administered only pharmaceuticals. Absence of IOP, is clarified by the fact that IOM is the mainly used contrast agent for radiographic examinations at the Radboudumc. Despite the frequent usage of antibiotics, DOX has not been detected in HSW and DSW, due to its limited stability and affinity

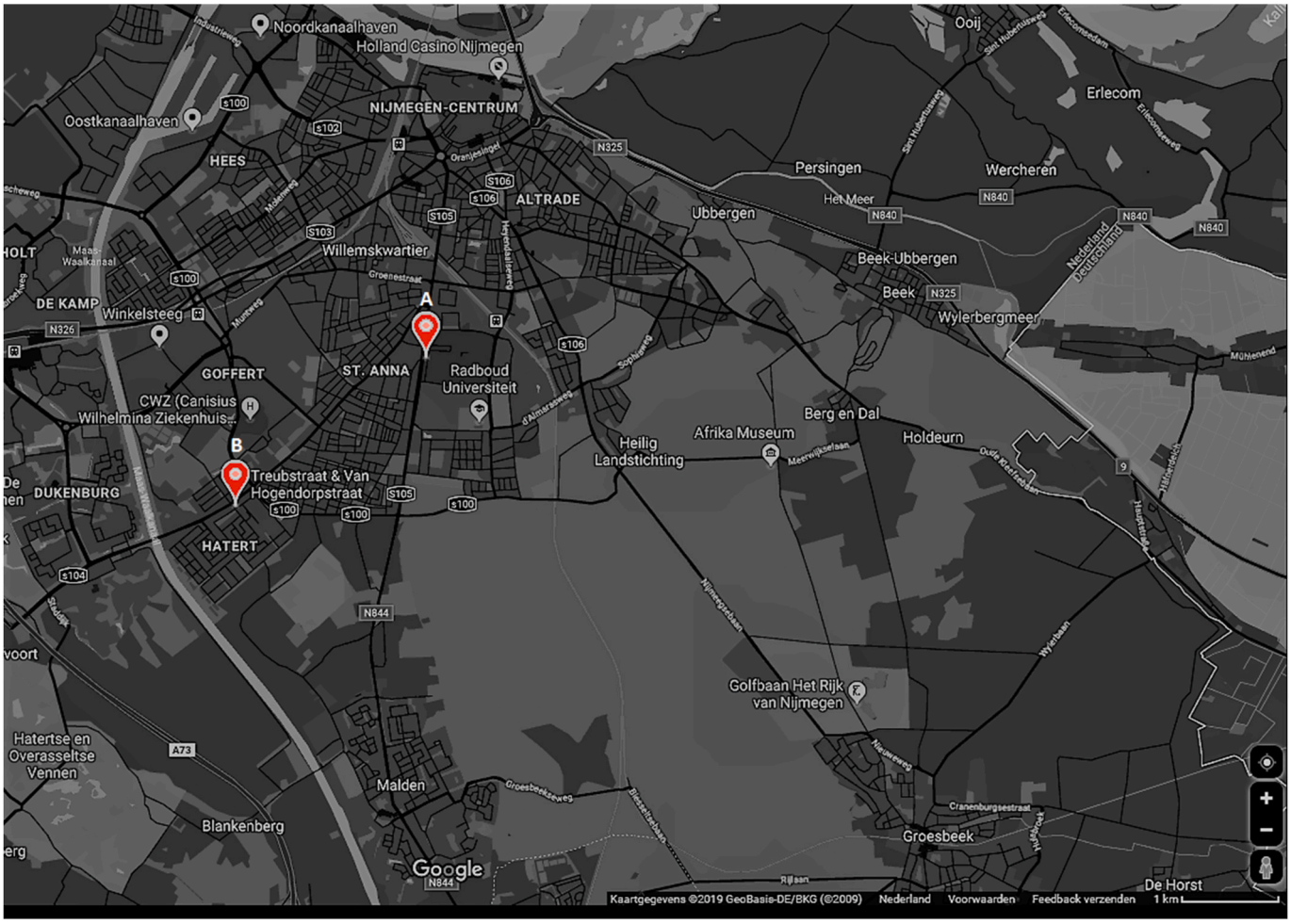

Fig. 6. Wastewater sampling points in the city of Nijmegen (the Netherlands). Sewage water was taken from a well at the Radboud University Medical Center **(A)** and in a residential area **(B)**. The sewer system of the end of pipe hospital effluent has no connection to the domestic sewage water well.

Table 4
Pharmaceutical detection in hospital sewage water compared to domestic sewage water in the city of Nijmegen.

Hospital sewage water (A) Thursday – Monday (12 - 16 Sep 2019, including a weekend) $\bar{x}$ Concentration (μg/L) (±sd) $n = 4$													
IOM[b]	IOP	DIA	DOX	CIP	FLU	DF	MET	CP	CB	TER	PHE	APAP	MF
2013.3 (±121.2)	n.d.	8.2 (±1.3)	n.d.	15.8 (±4.6)	0.16 (±0.05)	1.9 (±1.7)	0.97 (±0.14)	0.08 (±0.03)	0.15 (±0.09)	n.d.	n.d.	0.43[a]	30.1 (±13.6)
Hospital sewage water (A) Monday – Thursday (16 - 19 Sep 2019, working days) $\bar{x}$ Concentration (μg/L) (±sd) $n = 4$													
IOM	**IOP**	**DIA**	**DOX**	**CIP**	**FLU**	**DF**	**MET**	**CP**	**CB**	**TER**	**PHE**	**APAP**	**MF**
2387.3 (±190.9)	n.d.	10.1 (±1.9)	n.d.	14.5 (±4.9)	0.15 (±0.04)	3.1 (±3.6)	1.3 (±0.3)	0.34 (±0.10)	0.08 (±0.23)	n.d.	n.d.	82.1 (±81.9)	36.8 (±14.9)
Hospital sewage water (Pooled) $\bar{x}$ Concentration (μg/L) (±sd) $n = 2$													
IOM	**IOP**	**DIA**	**DOX**	**CIP**	**FLU**	**DF**	**MET**	**CP**	**CB**	**TER**	**PHE**	**APAP**	**MF**
2070.5 (±99.8)	n.d.	7.8 (±0.4)	n.d.	11.6 (±1.6)	0.20 (±0.02)	0.3 (±0.05)	1.2 (±0.08)	0.22 (±0.01)	0.17 (±0.10)	n.d.	n.d.	0.07[a] (±0.16)	19.0 (±1.6)
Domestic sewage water (B) Thursday (31 Oct 2019) $\bar{x}$ Concentration (μg/L) (±sd) $n = 4$													
IOM	**IOP**	**DIA**	**DOX**	**CIP**	**FLU**	**DF**	**MET**	**CP**	**CB**	**TER**	**PHE**	**APAP**	**MF**
n.d.	n.d.	n.d.	n.d.	1.1 (±0.5)	0.5 (±0.4)	5.6 (±4.7)	2.5 (±0.7)	n.d.	1.9 (±0.7)	n.d.	n.d.	482.9 [b] (±286.2)	76.4 (±30.0)

[a] It is recommended to analyse wastewater within 24h, to minimize biodegradation of APAP.
[b] Determined concentrations exceeding the calibration range were quantified by linear extrapolation using the corresponding slope and intercept prepared in synthetic sewage water.

for charged cations Ca^{2+} and Mg^{2+} (Soeborg et al., 2004; Loftsson 2014). Tetracycline antibiotics, such as DOX, are stable under acidic conditions but undergo chemical reactions at neutral and basic pH, like epimerization where hydroxyl and hydrogen group substituents exchange within the molecule by forming iso- or anhydrotetracyclines (Loftsson 2014). Tetracyclines predominantly absorb to sediment particles making it difficult to determine detectable amounts in wastewater samples (Thornton, 2001). That TER and PHE have not been found in the sewage water samples might be attributed to fact that other pharmaceuticals are used with the same therapeutic effect. Alternatives for TER and PHE are salbutamol and propyphenazone, molecules with very similar chemical properties and therapeutic effects (Zuehlke et al., 2007). Additionally, the route of discharge is also of importance, since concentrations of pharmaceuticals can vary per region. It is expected that the presence of TER is limited in urban sewage water samples, since the compound is mainly used as food additive in the veterinary sector to increase the amounts of lean meat of livestock (Zhou et al., 2017). The concentrations of pharmaceuticals detected in both HSW and DSW, provides qualitative information about their consumption. In the HSW it is worth mentioning the difference between the weekday and weekend sample, where the DSW sample reflects the continuous emission of prescription and over the counter medicines (Table 4).

3.6.1. Oxidative degradation chemistry in hospital sewage water

Previous pharmaceutical oxidative degradation results were obtained in a controlled setting. To evaluate the efficiency of plasma-induced water activation and UV-C/H_2O_2 on untreated hospital effluent, pharmaceutical decomposition of the 10 identified compounds was determined, see Fig. 7. The overall conversion levels for IOM, DIA, CIP, FLU, DF, MET, CP, CB, APAP and MF are all near equivalent to the results obtained in the synthetic sewage water matrix. This is remarkable since the determined concentrations for IOM (~2400 μg/L), DIA (~10 μg/L), CIP (~13 μg/L), APAP (~300 μg/L) and MF (~35 μg/L) were all much higher in HSW than in the spiked (5 μg/L) synthetic sewage water matrix, see Table S8 (SI **paragraph S10**). According to the controlled experimental results, it has become clear, that the efficiency of pharmaceutical degradation mainly depends on pH, matrix complexity and oxidative technique used. A high pharmaceutical concentration is also of influence, but primarily slows down the rate of chemical degradation (Graumans et al., 2019). That the high concentration of IOM with UV-C/H_2O_2 treatment decreases so rapidly, is attributed to its sensitivity to UV irradiation. To demonstrate effectiveness of both oxidative treatment techniques in hospital effluent, the total mass of the revealed pharmaceuticals was calculated according to a previously described method (Ajo et al., 2018). The overall conversion level was calculated with and without the contrast agents since the mass-based occurrence of IOM and DIA was relatively high compared to the other pharmaceuticals (Table 5).

According to the results provided in Table 5 and S8 (SI **paragraph S10**), it is suggested that thermal plasma treatment has the advantage over UV/H_2O_2 treatment, since in addition to ROS, also RNS are continuously produced in plasma activated water. With the exception of IOM and DIA, thermal plasma oxidative degradation proves its effectiveness in very complex matrices. The less gradual chemical degradation observed, during oxidative treatment in HSW is attributed to the matrix complexity. In our study only 10 compounds were detected in the HSW, but it is important to mention that many more analytes are to be expected (Ajo et al., 2018). Besides the pharmaceuticals that were not determined in this study, it is anticipated that molecules such as soaps, detergents, biotransformation products and hormones are also present in HSW. All these compounds will have an effect on the overall degradation efficiency e.g. competitive inhibition. The observed increase in sample concentration overtime for the analytes CP and CB is caused by their metabolites. During oxidative treatment, their non-detected

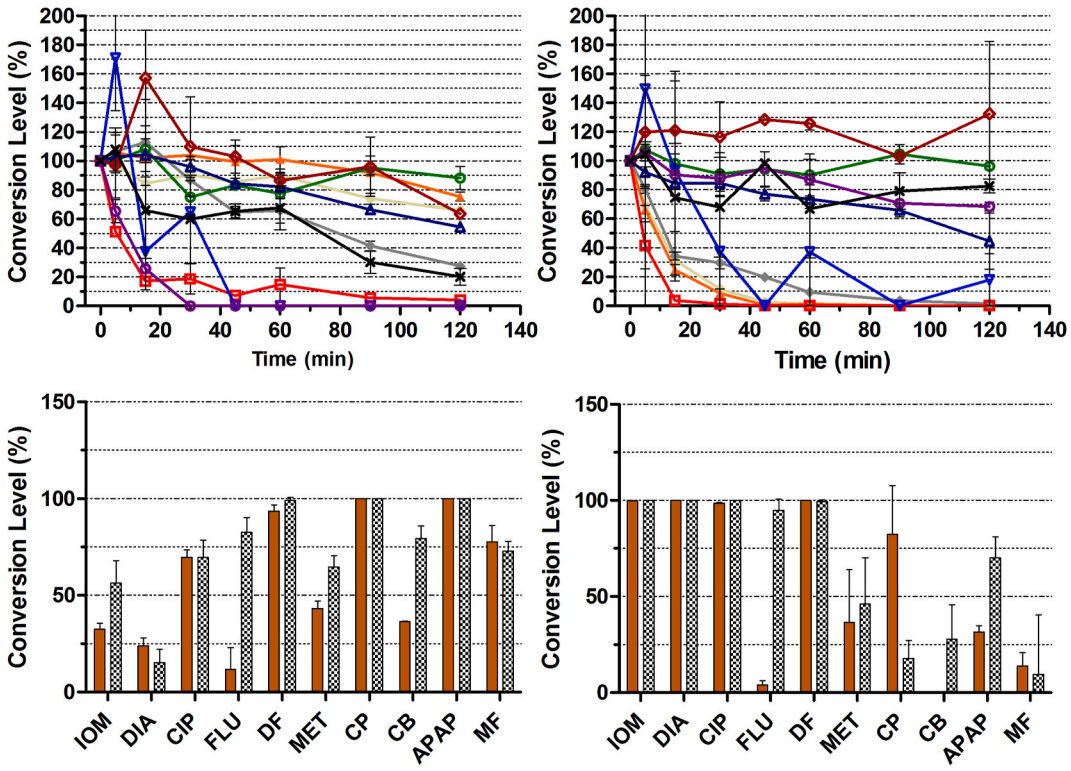

Fig. 7. Thermal plasma oxidation (**A**) was applied on hospital sewage water (HSW, $n = 3$). 10 compounds were identified, showing the conversion levels for; **IOM** (●, 32.5%), **DIA** (▲, 23.8%), **CIP**(◆, 69.7%), **FLU**(○, 11.8%), **DF** (□, 93.6%), **MET** (△, 43.3%), **CP**(▽, 100.0%), **CB**(◇, 36.4%), **APAP** (○, 100.0%), **MF**(✖, 77.7%). UV-C/H_2O_2 oxidative degradation (**B**) demonstrated; **IOM** (●, 99.9%), **DIA** (▲, 100.0%), **CIP**(◆, 98.6%), **FLU**(○, 4.0%), **DF** (□, 100.0%), **MET** (△, 36.5%), **CP**(▽, 82.3%), **CB** (◇, N.C), **APAP** (○, 31.6%), **MF**(✖, 13.9%). For both techniques the pharmaceutical decomposition in HSW (■) was compared to the controlled degradation results in synthetic sewage water (■). It is illustrated that both plasma oxidation (**C**) and UV-C/H_2O_2 (**D**) oxidative treatment in HSW initiate equivalent abatement as in the simulated matrix.

Table 5
Total identified pharmaceutical concentration in hospital sewage water, demonstrating the effectiveness of plasma oxidation and UV/H_2O_2 treatment with and without contrast agents.

AOP	Total Conc. pharmaceuticals (μg/L)	Removal (%)	Total Conc. w/o IOM and DIA (μg/L)	Removal (%) w/o IOM and DIA
Plasma $150W_{Start}$	2782.1	41.6	344.1	96.7
$End_{120\ min}$	1624.7		11.2	
UV-C/H2O2	2881.9	91.4	371.8	33.2
$End_{120\ min}$	248.5		248.3	

biological metabolites are reformed into the pristine structures. This will cause an increased peak value relative to the measured initial concentration. Continuation of the oxidative treatment will cause further abatement and make it possible to degrade the compound completely (Aziz et al., 2018; Ajo et al., 2018; Graumans et al., 2020).

3.7. Strengths and limitations of the study

We developed an experimental set-up to provide insight into the degradation of 14 pharmaceuticals in complex matrices by use of AOP. The application of plasma treatment compared to UV-C/H_2O_2 on simulated matrices, indicates dependency of the degradation efficiency on matrix complexity and also varies with the method of oxidative treatment and the structural properties of the pharmaceuticals tested. The simulation matrices were compared with end-of-pipe hospital sewage water, sampled and processed by advanced oxidation. Due to matrix complexity and an unexpected broad concentration range in real life wastewater our analytical approach for synthetic sewage water showed some limitations for quantification of pharmaceuticals like IOM and APAP. Additionally, our lowest calibration point (0.5 μg/L) did not optimally serve quantification of FLU, DF, CP and CB, since their determined concentrations ranged between the LOD and lowest calibration point in synthetic sewage water. Nonetheless, this laboratory study represents a useful first step in the experimental validation of plasma activation technology to complement onsite wastewater treatment.

4. Conclusion

With this study we have extensively studied the degradation of pharmaceuticals in multiple complex matrices using thermal plasma and UV/H_2O_2 oxidative treatment. Despite the matrix complexity has each

technique its own added value towards specific pharmaceutical classes. Single dose hydrogen peroxide in stationary UV-C/H_2O_2 treatment has a temporary effect, and involved photons cannot produce RNS, whereas ongoing plasma activation can produce both ROS and RNS continuously. The continuous production of reactive species makes plasma activation a useful technique for the application in complex matrices such as hospital effluent. The pharmaceutical degradation by temperature-controlled thermal plasma treatment is complemented by nitrification under acidic conditions. Further research using cell-based assays should reveal whether the toxicity of contaminated matrices is decreased.

Declaration of competing interest

The authors declare that they have no known competing financial interests or personal relationships that could have appeared to influence the work reported in this paper.

Acknowledgements

Financial support was made possible by the INTERREG Deutschland-Nederland program [grant number 142118]. The authors would like to thank VitalFluid who provided the PAW lab unit and UV-C source.

Appendix A. Supplementary data

Supplementary data to this article can be found online at https://doi.org/10.1016/j.envres.2021.110884.

References

Ajo, P., Preis, S., Vornamo, T., Manttari, M., Kallioinen, M., Louhi-Kultanen, M., 2018. Hospital wastewater treatment with pilot-scale pulsed corona discharge for removal of pharmaceutical residues (vol 6, pg 1569, 2018). J Environ Chem Eng 6 (2). https://doi.org/10.1016/j.jece.2018.06.013. A1-A1.

Allard, S., Criquet, J., Prunier, A., et al., 2016. Photodecomposition of iodinated contrast media and subsequent formation of toxic iodinated moieties during final disinfection with chlorinated oxidants. Water Res. 103, 453–461. https://doi.org/10.1016/j.watres.2016.07.050.

Almeida, A.M., Castel-Branco, M.M., Falcão, A.C., 2002. Linear regression for calibration lines revisited: weighting schemes for bioanalytical methods. J. Chromatogr. B 774, 215–222. https://doi.org/10.1016/S1570-0232(02)00244-1.

Aziz, K., Miessner, H., Mueller, S., et al., 2018. Comparative study on 2,4-dichlorophenoxyacetic acid and 2,4-dichlorophenol removal from aqueous solutions via ozonation, photocatalysis and non-thermal plasma using a planar falling film reactor. J. Hazard Mater. 343, 107–115. https://doi.org/10.1016/j.jhazmat.2017.09.025.

Banaschik, R., Lukes, P., Jablonowski, H., Hammer, M.U., Weltmann, K.D., Kolb, J.F., 2015. Potential of pulsed corona discharges generated in water for the degradation of persistent pharmaceutical residues. Water Res. 84, 127–135. https://doi.org/10.1016/j.watres.2015.07.018.

Banaschik, R., Jablonowski, H., Bednarski, P.J., Kolb, J.F., 2018. Degradation and intermediates of diclofenac as instructive example for decomposition of recalcitrant pharmaceuticals by hydroxyl radicals generated with pulsed corona plasma in water. J. Hazard Mater. 342, 651–660. https://doi.org/10.1016/j.jhazmat.2017.08.058.

Beier, S., Koster, S., Veltmann, K., Schroder, H., Pinnekamp, J., 2010. Treatment of hospital wastewater effluent by nanofiltration and reverse osmosis. Water Sci. Technol. 61 (7), 1691–1698. https://doi.org/10.2166/wst.2010.119.

Borowska, E., Felis, E., Zabczynski, S., 2015. Degradation of iodinated contrast media in aquatic environment by means of UV, UV/TiO2 process, and by activated sludge. Water, Air, Soil Pollut. 226 (5). ARTN 15110.1007/s11270-015-2383-9.

Bourin, M., Jolliet, P., Ballereau, F., 1997. An overview of the clinical pharmacokinetics of x-ray contrast media. Clin. Pharmacokinet. 32 (3), 180–193. https://doi.org/10.2165/00003088-199732030-00002.

Brisset, J.L., Benstaali, B., Moussa, D., Fanmoe, J., Njoyim-Tamungang, E., 2011. Acidity control of plasma-chemical oxidation: applications to dye removal, urban waste abatement and microbial inactivation. Plasma Sources Sci. Technol. 20 (3) https://doi.org/10.1088/0963-0252/20/3/034021. Artn 034021.

Brown, T.L., Bursten, B.E., Langford, S., Sagatys, D., Duffy, 2007. Alkenes, Alkynes and Arenes Chemistry. The central science a broad perspectivePearson Education Australia, French Forest, pp. 888–937.

Chiron, S., Gomez, E., Fenet, H., 2010. Nitration processes of acetaminophen in nitrifying activated sludge. Environ. Sci. Technol. 44 (1), 284–289. https://doi.org/10.1021/es902129c.

Eloy, R., Corot, C., Belleville, J., 1991. Contrast media for angiography: physicochemical properties, pharmacokinetics and biocompatibility. Clin. Mater. 7 (2), 89–197. https://doi.org/10.1016/0267-6605(91)90045-h.

Ferrando-Climent, L., Rodriguez-Mozaz, S., Barcelo, D., 2014. Incidence of anticancer drugs in an aquatic urban system: from hospital effluents through urban wastewater to natural environment. Environ. Pollut. 193, 216–223. https://doi.org/10.1016/j.envpol.2014.07.002.

Gerrity, D., Stanford, B.D., Trenholm, R.A., Snyder, S.A., 2010. An evaluation of a pilot-scale nonthermal plasma advanced oxidation process for trace organic compound degradation. Water Res. 44 (2), 493–504. https://doi.org/10.1016/j.watres.2009.09.029.

Giannakis, S., Androulaki, B., Comninellis, C., Pulgarin, C., 2018. Wastewater and urine treatment by UVC-based advanced oxidation processes: implications from the interactions of bacteria, viruses, and chemical contaminants. Chem. Eng. J. 343, 270–282. https://doi.org/10.1016/j.cej.2018.03.019.

Graumans, M.H.F., Hoeben, W., Russel, F.G.M., Scheepers, P.T.J., 2020. Oxidative degradation of cyclophosphamide using thermal plasma activation and UV/H2O2 treatment in tap water. Environ. Res. 182, 109046. https://doi.org/10.1016/j.envres.2019.109046.

Gu, H., Liu, G., Wang, J., Aubry, A.F., Arnold, M.E., 2014. Selecting the correct weighting factors for linear and quadratic calibration curves with least-squares regression algorithm in bioanalytical LC-MS/MS assays and impacts of using incorrect weighting factors on curve stability, data quality, and assay performance. Anal. Chem. 86 (18), 8959–8966. https://doi.org/10.1021/ac5018265.

Hoeben, W.F.L.M., van Ooij, P.P., Schram, D.C., Huiskamp, T., Pemen, A.J.M., Lukes, P., 2019. On the possibilities of straightforward characterization of plasma activated water. Plasma Chem. Plasma Process. 39 (3), 597–626. https://doi.org/10.1007/s11090-019-09976-7.

Jeong, J., Jung, J., Cooper, W.J., Song, W., 2010. Degradation mechanisms and kinetic studies for the treatment of X-ray contrast media compounds by advanced oxidation/reduction processes. Water Res. 44 (15), 4391–4398. https://doi.org/10.1016/j.watres.2010.05.054.

Jewell, K.S., Wick, A., Ternes, T.A., 2014. Comparisons between abiotic nitration and biotransformation reactions of phenolic micropollutants in activated sludge. Water Res. 48, 478–489. https://doi.org/10.1016/j.watres.2013.10.010.

Joshi, R.P., Thagard, S.M., 2013. Streamer-like electrical discharges in water: Part II. Environmental applications. Plasma Chem. Plasma Process. 33 (1), 17–49. https://doi.org/10.1007/s11090-013-9436-x.

Kohler, C., Venditti, S., Igos, E., Klepiszewski, K., Benetto, E., Cornelissen, A., 2012. Elimination of pharmaceutical residues in biologically pre-treated hospital wastewater using advanced UV irradiation technology: a comparative assessment. J. Hazard Mater. 239–240, 70–77. https://doi.org/10.1016/j.jhazmat.2012.06.006.

Li, Y., Niu, X.M., Yao, C., Yang, W., Lu, G.H., 2019. Distribution, removal, and risk assessment of pharmaceuticals and their metabolites in five sewage plants. Int. J. Environ. Res. Publ. Health 16 (23). ARTN 472910.3390/ijerph16234729.

Lin, W.T., Zhang, X.H., Li, P., Tan, Y.Z., Ren, Y., 2020. Ultraviolet photolysis of metformin: mechanisms of environmental factors, identification of intermediates, and density functional theory calculations. Environ. Sci. Pollut. Res. 27 (14), 17043–17053. https://doi.org/10.1007/s11356-020-08255-9.

Loftsson, T., 2014. Tetracyclines Drug Stability for Pharmaceutical Scientists.

Magureanu, M., Mandache, N.B., Parvulescu, V.I., 2015. Degradation of pharmaceutical compounds in water by non-thermal plasma treatment. Water Res 81, 124–136. https://doi.org/10.1016/j.watres.2015.05.037.

Magureanu, M., Bradu, C., Parvulescu, V.I., 2018. Plasma processes for the treatment of water contaminated with harmful organic compounds. J. Phys. D Appl. Phys. 51 (31) https://doi.org/10.1088/1361-6463/aacd9c. ARTN 313002.

Markovic, M., Jovic, M., Stankovic, D., Kovacevic, V., Roglic, G., Gojgic-Cvijovic, G., Manojlovic, D., 2015. Application of non-thermal plasma reactor and Fenton reaction for degradation of ibuprofen. Sci. Total Environ. 505, 1148–1155. https://doi.org/10.1016/j.scitotenv.2014.11.017.

Miller, J.N., Miller, J.C., 2010. Statistics and Chemometrics for Analytical Chemistry. Pearson, pp. 110–153.

OECD, 2001. OECD GUIDELINE for the TESTING of CHEMICALS Simulation Test - Aerobic Sewage Treatment: 303 A: Activated Sludge Units - 303 B: Biofilms. https://www.oecd-ilibrary.org/.

Peake, B.M., Braund, R., Tong, A.Y.C., Tremblay, L.A., 2016. The Life-Cycle of Pharmaceuticals in the Environment. Woodhead Publishing, Cambridge, United Kingdom.

Pemen, A.J.M., van Ooij, P.P., Beckers, F.J.C.M., et al., 2017. Power modulator for high-yield production of plasma-activated water. Ieee T Plasma Sci 45 (10), 2725–2733. https://doi.org/10.1109/Tps.2017.2739484.

Petrie, B., Youdan, J., Barden, R., Kasprzyk-Hordern, B., 2016. Multi-residue analysis of 90 emerging contaminants in liquid and solid environmental matrices by ultra-high-performance liquid chromatography tandem mass spectrometry. J. Chromatogr. A 1431, 64–78. https://doi.org/10.1016/j.chroma.2015.12.036.

Rosati, G., 1994. Clinical-pharmacology of iomeprol. Eur. J. Radiol. 18, S51–S60. https://doi.org/10.1016/0720-048x(94)90094-9.

Shih, K.Y., Locke, B.R., 2011. Optical and electrical diagnostics of the effects of conductivity on liquid phase electrical discharge. Ieee T Plasma Sci 39 (3), 883–892. https://doi.org/10.1109/Tps.2010.2098052.

Shimizu, T., Kishimoto, N., Sato, T., 2020. Effect of electrical conductivity of water on plasma-driven gas flow by needle-water discharge at atmospheric pressure. J. Electrost. 104. ARTN 10342210.1016/j.elstat.2020.103422.

Soeborg, T., Ingerslev, F., Halling-Sorensen, B., 2004. Chemical stability of chlortetracycline and chlortetracycline degradation products and epimers in soil interstitial water. Chemosphere 57 (10), 1515–1524. https://doi.org/10.1016/j.chemosphere.2004.09.020.

Souza, F.S., Feris, L.A., 2016. Hospital and municipal wastewater: identification of relevant pharmaceutical compounds. Water Environ. Res. 88 (9), 871–877. https://doi.org/10.2175/106143016X14609975747603.

Squadrito, G.L., Pryor, W.A., 1998. Oxidative chemistry of nitric oxide: the roles of superoxide, peroxynitrite, and carbon dioxide. Free Radic. Biol. Med. 25 (4–5), 392–403. https://doi.org/10.1016/s0891-5849(98)00095-1.

Suarez, S., Lema, J.M., Omil, F., 2009. Pre-treatment of hospital wastewater by coagulation-flocculation and flotation. Bioresour. Technol. 100 (7), 2138–2146. https://doi.org/10.1016/j.biortech.2008.11.015.

Thirumdas, R., Kothakota, A., Annapure, U., et al., 2018. Plasma activated water (PAW): chemistry, physico-chemical properties, applications in food and agriculture. Trends Food Sci. Technol. 77, 21–31. https://doi.org/10.1016/j.tifs.2018.05.007.

Thornton, L., Butler, D., Docx, P., Hession, M., Makropoulos, C., McMullen, M., Nieuwenhuijsen, M., Pitman, A., Rautiu, R., Sawyer, R., Smith, S., White, D., Wilderer, P., Paris, S., Marani, D., Braguglia, C., Palerm, J., 2001. Pollutants in Urban Waste Water and Sewage Sludge. European Commission, Luxembourg.

Tokumura, M., Sugawara, A., Raknuzzaman, M., Habibullah-Al-Mamun, M., Masunaga, S., 2016. Comprehensive study on effects of water matrices on removal of pharmaceuticals by three different kinds of advanced oxidation processes. Chemosphere 159, 317–325. https://doi.org/10.1016/j.chemosphere.2016.06.019.

Vieno, N.M., Tuhkanen, T., Kronberg, L., 2006. Analysis of neutral and basic pharmaceuticals in sewage treatment plants and in recipient rivers using solid phase extraction and liquid chromatography-tandem mass spectrometry detection. J. Chromatogr. A 1134 (1–2), 101–111. https://doi.org/10.1016/j.chroma.2006.08.077.

von Sonntag, C., 2008. Advanced oxidation processes: mechanistic aspects. Water Sci. Technol. 58 (5), 1015–1021. https://doi.org/10.2166/wst.2008.467.

Wang, Y.F., Roddick, F.A., Fan, L.H., 2017. Direct and indirect photolysis of seven micropollutants in secondary effluent from a wastewater lagoon. Chemosphere 185, 297–308. https://doi.org/10.1016/j.chemosphere.2017.06.122.

Wols, B.A., Hofman-Caris, C.H., Harmsen, D.J., Beerendonk, E.F., 2013. Degradation of 40 selected pharmaceuticals by UV/H2O2. Water Res. 47 (15), 5876–5888. https://doi.org/10.1016/j.watres.2013.07.008.

Yin, J., Yang, Y., Li, K., Zhang, J., Shao, B., 2010. Analysis of anticancer drugs in sewage water by selective SPE and UPLC-ESI-MS-MS. J. Chromatogr. Sci. 48 (10), 781–789. https://doi.org/10.1093/chromsci/48.10.781.

Yoshida, M., Akane, A., 1999. Subzero-temperature liquid-liquid extraction of benzodiazepines for high performance liquid chromatography. Anal. Chem. 71 (9), 1918–1921. https://doi.org/10.1021/ac981276g.

Zhao, C., Arroyo-Mora, L.E., DeCaprio, A.P., Sharma, V.K., Dionysiou, D.D., O'Shea, K.E., 2014. Reductive and oxidative degradation of iopamidol, iodinated X-ray contrast media, by Fe(III)-oxalate under UV and visible light treatment. Water Res. 67, 144–153. https://doi.org/10.1016/j.watres.2014.09.009.

Zhou, L., Sleiman, M., Ferronato, C., Chovelon, J.M., de Sainte-Claire, P., Richard, C., 2017. Sulfate radical induced degradation of beta 2-adrenoceptor agonists salbutamol and terbutaline: phenoxyl radical dependent mechanisms. Water Res. 123, 715–723. https://doi.org/10.1016/j.watres.2017.07.025.

Zuehlke, S., Duennbier, U., Heberer, T., 2007. Investigation of the behavior and metabolism of pharmaceutical residues during purification of contaminated ground water used for drinking water supply. Chemosphere 69 (11), 1673–1680. https://doi.org/10.1016/j.chemosphere.2007.06.020.